

INTERACTION OF LASER RADIATION WITH MATTER. LASER PLASMA https://doi.org/10.1070/QEL16674

Generation of X-ray radiation from a plasma in a microchannel of a copper target located in the air under the action of soft-focused femtosecond laser pulses with an intensity of 100 TW cm^{-2}

A.A. Garmatina, I.A. Zhvaniya, F.V. Potemkin, V.M. Gordienko

Abstract. **We have studied the dependence of X-ray radiation yield in the range of more than 3 keV from a microchannel in a copper target on the laser pulse number at a (0.7–4.0) × 10^{14} W cm^{-2} intensities of femtosecond laser radiation. A technique for estimating the intensity of laser radiation acting on the target using the slope of the X-ray bremsstrahlung spectrum is proposed. A possibility of using this technique for estimating the intensity in a femtosecond laser filament is considered.**

Keywords: *X-ray radiation, femtosecond plasma, laser ablation, hot electrons.*

1. Introduction

The interaction of intense femtosecond laser pulses with a solid target in the microplasma generation regime is the subject of active research [1], for example, in precision microprocessing of materials [2], real-time contactless diagnostics of the elemental composition of matter by the technique of laser-induced breakdown spectroscopy [3], and formation of X-ray [4] and THz [5] sources. It is well known that the interaction of high-intensity femtosecond laser radiation ($I > 10^{15}$ W cm^{-2}) with a solid target leads to the formation of a dense plasma with a concentration of free-electrons $N_e \approx 10^{23}$ cm^{-3}, representing a source of X-ray photons with an energy of more than 3 keV. However, even at lower intensities ($\sim 10^{14}$ W cm^{-2}), the existence of hot electrons with an energy of 1.5–2.0 keV in the microplasma initiates generation of X-ray radiation [6], whose yield depends on the ultrashort pulse duration (its optimum value varies with the target material). As example, for a copper target, the optimum pulse duration, at which the X-ray radiation yield attains its maximum, is about 200 fs [4].

A new regime of microplasma initiation in the near-surface region of a solid target placed in vacuum arises when a sequence of femtosecond laser pulses with an intensity of more than 100 TW cm^{-2} acts upon a target at tight focusing (NA ~ 0.2). In this case, as a result of ablation, conical microchannels are formed, in which the intensity I increases due to the light flux concentration, the energy of hot electrons rises, and, accordingly, the yield of X-ray radiation with photon energy up to 20 keV increases [7]. When the target is placed in the air, the ionisation of molecular components and the appearance of an electron cloud may reduce the X-ray yield and the energy of hot electrons due to the nonlinear energy losses and as a result of self-defocusing [8, 9]. It is known, however, that at intensities up to 4.0 × 10^{14} W cm^{-2} and operating wavelength of 0.8 μm, the nonlinear energy losses for ionisation in the air do not exceed 10% [10, 11]. The use of longer-wavelength laser radiation can reduce ionisation losses [12], and the transition to the soft-focusing regime (NA ~ 0.02–0.03) allows ionisation losses to be minimised [11] even at relatively high laser pulse energy (within 1 mJ). In addition, due to the formation of a comparatively long beam waist in the case of soft focusing, the target position relative to the focal plane is not critical. In comparison with the tight focusing regime, this should provide a more efficient control over the microchanneling process by the X-ray feedback signal, which is important, for example, in monitoring the formation of microchannels in multilayer targets or biological objects [13].

Thus, the repetition rate regime of femtosecond laser pulse impact on the target in the soft-focusing regime allows generation of a sequence (package) of X-ray pulses in the process of microchannel formation in the target. This can be employed to form a X-ray source (bremsstrahlung and characteristic radiation), to estimate the radiation intensity, and also to monitor the process of microchannel formation. It is significant that the use of a longer-wavelength femtosecond laser radiation compared to the traditionally used radiation of a Ti:sapphire laser (0.8 μm) is more efficient (at comparable intensities) for the X-ray generation due to quadratic dependence of the average energy of hot electrons on the wavelength [14].

The aim of the present work is to investigate the dependence of the laser energy conversion efficiency (in the range of more than 3 keV) on the number of a femtosecond laser pulse (near-IR radiation with 1.24 μm wavelength, pulse duration of 200 fs) which are softly focused on the surface of a copper target in the air (NA = 0.03) with an intensity of about 100 TW cm^{-2}, and to analyse the possibility of estimating the laser radiation intensity using the X-ray energy spectrum.

A.A. Garmatina Faculty of Physics, M.V. Lomonosov Moscow State University, Vorob'evy Gory, 119991 Moscow, Russia; National Research Center 'Kurchatov Institute', pl. Akad. Kurchatova 1, 123182 Moscow, Russia; e-mail: alga009@mail.ru;
I.A. Zhvaniya, V.M. Gordienko Faculty of Physics, M.V. Lomonosov Moscow State University, Vorob'evy Gory, 119991 Moscow, Russia;
F.V. Potemkin Faculty of Physics, M.V. Lomonosov Moscow State University, Vorob'evy Gory, 119991 Moscow, Russia; International Laser Center, M.V. Lomonosov Moscow State University, Vorob'evy Gory, 119991 Moscow, Russia

Received 7 April 2018; revision received 22 May 2018
Kvantovaya Elektronika **48** (7) 648–652 (2018)
Translated by M.A. Monastyrskiy

2. Experiment

In our experiments (the scheme of the setup is shown in Fig. 1), we used a femtosecond Cr : forsterite laser with a radiation wavelength $\lambda = 1.24$ μm, a pulse duration of 200 fs (as noted above, this value is optimal for X-ray generation in a copper target [4]) and a pulse repetition rate of 10 Hz. The pulse energy did not exceed 1 mJ; the laser energy contrast on the nanosecond scale was about 300. The radiation was focused on the target surface using a lens with a focal length $f = 30$ cm, which corresponds to a numerical aperture NA = 0.03. A copper foil with a thickness of 80 μm, glued to the glass substrate, was chosen as a target. The time moment of the foil breakdown in the glass substrate after subsequent ignition of plasma was controlled visually. Proceeding from the time moment of the plasma occurrence, it was possible to find the average rate of the foil ablation. The focal beam diameter, which was determined as the average of the diameter of a crater formed in the glass plate by two-to-five laser pulses in the range of operating intensities $(0.7-4.0) \times 10^{14}$ W cm^{-2}, appeared to be 40 μm. The radiation was focused at normal incidence to the target surface. For comparative experiments in the air and vacuum (with residual pressure of 0.01 Torr), the target was located in the chamber at an angle of 45° to the direction of laser radiation propagation.

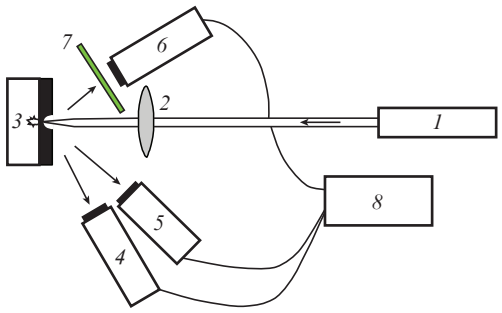

Figure 1. Scheme of the setup:
(*1*) femtosecond Cr : forsterite laser; (*2*) lens; (*3*) copper target on a substrate; (*4*) PMT_X-ray; (*5*) Amptek X-ray spectrometer; (*6*) optical photomultiplier; (*7*) set of optical filters; (*8*) PC.

To measure the X-ray integral yield, a 9107FLB photomultiplier tube (hereinafter PMT_X-ray) equipped with a NaI(Tl) scintillator was used. A beryllium filter with a thickness of 180 μm was installed at the PMT_X-ray input. A calibrated X-ray detector provided the recording of the total X-ray energy in the range from 18 keV (or 2.9 fJ, which corresponds to the instrument noise level) to 8 MeV (1.3 pJ) in each laser shot. The PMT_X-ray was located at an angle of approximately 45° to the direction of laser radiation propagation with a distance of 7 cm from the target. With the X-ray absorption by the beryllium filter and by air taken into account, the PMT_X-ray was recording photons with energies of more than 3 keV. The recording of plasma radiation in the optical range was performed by PMT. The linearity of its operation regime was determined by IR and ND glass filters. Synchronous launching of the PMT_X-ray and optical PMT was programmed; therefore, the appearance of a signal from the optical photomultiplier coincided with the appearance of the laser-induced plasma on the target surface. This scheme made it possible to capture the pulse number at which the X-ray generation occurs. The X-ray spectrum was measured in the energy range of 3–18 keV by an Amptek spectrometer located at a distance of 8 cm from the target. The single-quantum operating regime of the spectrometer was provided by an aperture with a diameter of 0.5 mm, installed in front of the spectrometer. The spectrometer was calibrated by a source based on the Fe-55 ferrum isotope. The number of X-ray photons per pulse per solid angle was found as

$$N_2 = N_1 \frac{4\pi R_2^2}{\pi R_1^2 T},$$

where R_1 is the aperture radius; R_2 is the distance from the target to the spectrometer input window; N_1 is the number of registered quanta; and T is the filter transmittance.

The choice of the target material was determined by the fact that copper is widely used for similar studies and has a characteristic line with an energy of 8 keV, which falls into the recording region of the PMT_X-ray and Amptek spectrometer. The relatively small foil thickness made it possible to estimate the average ablation rate and ignore the peculiarities associated with the X-ray absorption by the target material on the way to the recording device.

3. Experimental results

At the first stage, we determined the laser radiation intensity, at which the presence of an air medium did not affect the X-ray yield due to the absence of losses caused by nonlinear absorption of radiation in the air. To this end, comparative experiments were conducted to measure the dependence of the total energy of X-ray photons emitted from the microchannel of a copper target located in the air and vacuum on the laser pulse number. The total X-ray energy from the microchannel plasma over the first five pulses was calculated (during this time a deep microchannel is not yet formed, and it can be assumed that the laser radiation interacts with the target surface). The coincidence of the total X-ray yield in the case of air and vacuum within the measurement error was observed up to the laser radiation intensity of 2×10^{14} W cm^{-2}. At $I = (4.0 \pm 0.2) \times 10^{14}$ W cm^{-2}, the losses for nonlinear absorption did not exceed 10%. Thus, for $I < (4.0 \pm 0.2) \times 10^{14}$ W cm^{-2}, the losses due to nonlinear absorption in the air can be neglected. Below, the experiments were conducted within this range.

The next step was to determine the X-ray generation threshold and to study the signal variation dynamics in the microchannel of the copper target as a function of the laser radiation intensity. The minimum intensity on the target surface, at which it was possible to record the X-rays from the target's microchannel was $(0.7 \pm 0.1) \times 10^{14}$ W cm^{-2}. The threshold intensity, at which the X-rays were recorded already in the first pulse (interaction with the unmodified target surface) was $(1.2 \pm 0.2) \times 10^{14}$ W cm^{-2}. The X-ray yield dependence on the pulse number n is shown in Fig. 2 for three intensities: minimum intensity $(0.7 \pm 0.1) \times 10^{14}$ W cm^{-2}, threshold intensity $(1.2 \pm 0.2) \times 10^{14}$ W cm^{-2}, and maximum intensity $(4.0 \pm 0.2) \times 10^{14}$ W cm^{-2}. The moving average method was employed to average the dependences of the total X-ray energy emitted from plasma in the target microchannel on the pulse number, which allowed us to approximate the obtained data by a nonlinear function. It was found that the X-ray

energy has a power-like dependence ($E = C + E_0 n^{\alpha}$) on the laser pulse number n. At an intensity of $(0.7 \pm 0.1) \times 10^{14}$ W cm^{-2}, the power exponent is $\alpha_1 = 2.9 \pm 0.1$ ($E_0 = 3.4 \times 10^{-6}$), at an intensity of $(1.2 \pm 0.2) \times 10^{14}$ W cm^{-2}, the power exponent decreases to $\alpha_2 = 2.3 \pm 0.1$ ($E_0 = 2.9 \times 10^{-4}$), while at an intensity of $(4.0 \pm 0.2) \times 10^{14}$ W cm^{-2}, we have $\alpha_3 = 1.9 \pm 0.1$ ($E_0 = 0.08$). This behaviour of α seems to be related to different initial conditions of the channel formation. At low and threshold intensities, the channel formation in the initial stages is slow, and only to the 70th pulse approximately the X-ray signal starts to grow due to an increase in intensity as a result of the channel narrowing and an increase in the ablation rate.

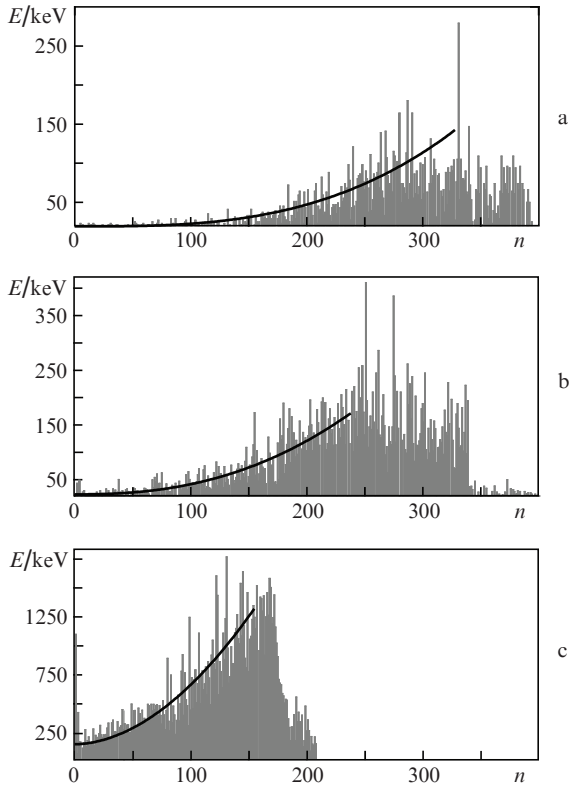

Figure 2. Spectrum-integrated energy E of X-ray quanta recorded using the PMT_X-ray from plasma in the target microchannel as a function of the laser pulse number n at (a) $I \approx (0.7 \pm 0.1) \times 10^{14}$, (b) $(1.20 \pm 0.15) \times 10^{14}$ and (c) $(4.0 \pm 0.2) \times 10^{14}$ W cm^{-2}.

At the maximum intensity $(4.0 \pm 0.2) \times 10^{14}$ W cm^{-2}, the picture changes dramatically, and the X-ray signal starts to grow from the first pulses. A decrease in the coefficient α is accompanied by an increase in the coefficient E_0; therefore, Fig. 2c shows the highest growth rate of the signal in the entire range n. Using the data on the time interval required for the target perforation and the target thickness (80 μm), the average ablation rate for the intensity range used can be estimated as 0.18–0.5 μm pulse^{-1}. This is consistent with the ablation rate data for the femtosecond laser radiation wavelength of 0.8 μm given in [10]. We also note that an increase in the coefficient E_0 with a change in the laser radiation intensity reflects (albeit nonlinearly) an increase in the average ablation rate.

As the laser radiation intensity on the target surface increases, the ablation rate increases as well. Thus, the pulse number begins to decrease, starting from which the X-ray yield grows significantly and the coefficient α decreases. We associate the presence of the X-ray yield maximum with the concentration (subfocusing) of radiation in the conical channel and, accordingly, with the growth in the I value. After reaching the maximum intensity, the X-ray yield remains quasi-constant until a through hole is formed (signal saturation interval, Figs 2a and 2b). This may be due to the appearance of a number of processes competing with subfocusing: as the microchannel depth increases and, consequently, the X-ray radiation source, located at the channel bottom, deepens and the transport path length in the probing direction increases. This results in the absorption of the X-ray signal recorded in the target volume. In addition, a suspension of the target material can be formed in the channel [15], which leads to additional absorption of X-ray radiation, plasma shielding of laser radiation inside the channel, and stabilisation of its diameter.

A sharp drop in the X-ray yield (Fig. 2c) is caused by the target perforation. A reduction in the laser beam diameter within the channel is also confirmed by the fact that the output aperture size is, as a rule, smaller than the input one. We note that, in experiments with a thicker target (500 μm), after reaching the maximum amplitude of the signal and its stabilisation at a certain level, the X-ray signal decreases exponentially. We believe that the nature of this phenomenon is determined by the described X-ray absorption processes in the target volume and an increase in the amount of suspended matter within the channel. We also note that, if the focal waist is less than the target thickness, the X-ray signal starts to decrease due to the laser beam defocusing. Similar behaviour of the X-ray yield from the channel was observed by us earlier with a tighter focusing [16].

Note that if the laser radiation intensity is greater than the threshold one, the X-ray signal in the first pulses is characterised by a jump in its amplitude. Herewith, the X-ray yield in the first pulse exceeds the corresponding value in the next two to five pulses by about two times at $I \approx 10^{14}$ W cm^{-2} (Fig. 2b) and by about four times at $I \approx 4 \times 10^{14}$ W cm^{-2} (Fig. 2c). Thus, at the intensity close to the maximum intensity for this experiment, the intensity of the radiation incident on the target surface is comparable to the maximum intensity in the channel.

The data obtained made it possible to construct the total X-ray integral yield for the first and second laser pulses acting on the target surface as a function of intensity (Fig. 3a). It was found that these dependences can be approximated by the power-like function $E \sim E_0 I^{\gamma}$ [17], where in the case of the first laser pulse, the power exponent is $\gamma_1 = 3.5$, while for the second pulse $\gamma_2 = 2.5$ (Fig. 3a). An increase in the X-ray energy for the first pulse with normal radiation incidence onto the target can be related to interference of the incident radiation and the radiation reflected from the surface. As can be seen from Fig. 3a, the contribution of this effect increases with intensity I. The presence of the interference process is also confirmed by the fact that there is no jump in the X-ray signal for the first pulse when the laser radiation is focused onto the target obliquely.

The X-ray yield dependence on the laser radiation intensity for the second pulse makes it possible to estimate the increase in I in the target channel. The amplitude of the second pulse is used for such estimation, since for that pulse the interference effect should disappear due to the microcrater appearance. Given that the minimum X-ray yield value differs from the maximum one by approximately 5–7 times, the

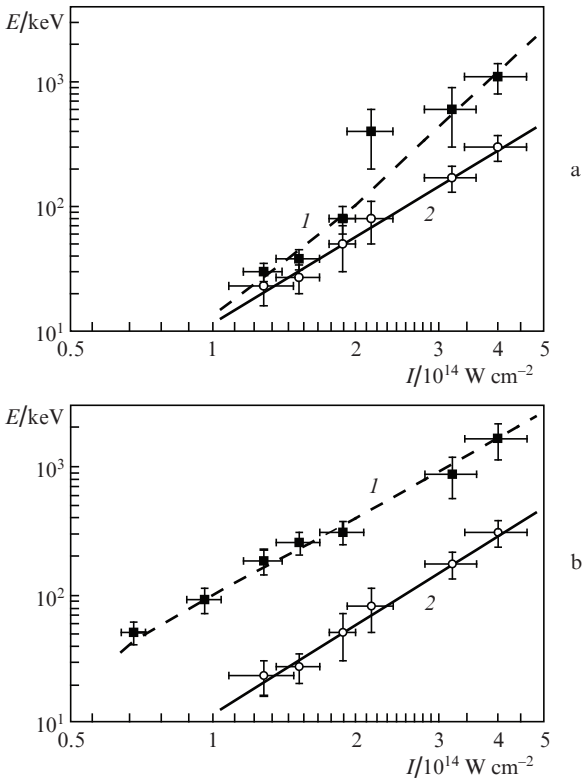

Figure 3. (a) Total energy of X-ray quanta recorded using the PMT_X-ray in the (*1*) first and (*2*) second pulses and also (b) the maximal integral energy of X-ray quanta emitted from plasma (*1*) in the microchannel recorded using the PMT_X-ray and (*2*) in the second pulse as functions of the laser radiation intensity.

intensity in the target microchannel should increase by no more than 2 times, and the beam diameter can decrease by approximately 1.4 times.

The dependence of the X-ray maximum yield from plasma in the microchannel on the I value in the range $(0.7-4.0) \times 10^{14}$ W cm^{-2} is approximated by a function with a power exponent $\gamma_3 = 2.2$ (Fig. 3b, solid line). At $I \approx 10^{14}$ W cm^{-2}, the amplitudes of the X-ray signal from plasma in the microchannel exceed by about 7 times the minimum amplitude of the X-rays initiated by the incident radiation, and by about 5 times at $I \approx 4 \times 10^{14}$ W cm^{-2}. This may be stipulated by a decrease in the microchannel aspect ratio with an increase in the radiation intensity acting on the target.

Thus, it was established that the threshold intensity on the target surface in the air, at which X-ray generation from plasma in the microchannel is possible is below the threshold intensity that is required for X-ray generation from the near-surface plasma, and constitutes 0.7×10^{14} W cm^{-2}. The dependence of the X-ray yield from the microchannel plasma on the laser pulse number has the form of a power-like function whose exponent is determined by the incident radiation intensity.

The obtained X-ray yield dependence from the target surface on the I value, also approximated by a power-like function, allowed us to estimate the increase in intensity I in the microchannel, which did not exceed three times.

X-ray spectra can be informative for characterisation of laser plasma parameters and for additional estimation of the intensity of incident radiation.

It is known that the measured X-ray bremsstrahlung spectrum can be used to estimate the average energy T_{hot} of hot electrons [15]: $Y_{x-ray} \cong (\beta/\sqrt{T_{hot}})\exp(-\mathcal{E}/T_{hot})$, where β is the coefficient depending on the plasma parameters, and $\mathcal{E}$ is the energy of X-ray quanta in keV.

In the case of resonant absorption of laser radiation energy by plasma (which is typical for experimental conditions), the average energy of hot electrons is related to the intensity I and the wavelength λ of incident radiation by the expression [14, 17]: $T_{hot} \cong A(I\lambda^2)^{1/3}$, where A is the proportionality coefficient. Thus, having determined the average energy of hot electrons, we can estimate the intensity of incident radiation.

It was established in [14] that, at $I \approx 10^{16}$ W cm^{-2} for measurements in vacuum $A = 5.3 \pm 0.2$. In order to refine this coefficient in the T_{hot} dependence for the conditions of our experiment, the X-ray spectrum of the microchannel plasma was measured in the regime of a transversely moving copper target (to attain the required signal-to-noise ratio) at $I \approx 3 \times 10^{14}$ W cm^{-2} (Fig. 4). In this case, the maximum X-ray yield from the microchannel is approximately 3 times greater than the minimum X-ray value for the second pulse from the pulse train (see Fig. 3b). This increase corresponds to the growth in intensity (with taking into account the previously established relation $E \sim I^{2.5}$) by about 1.5 times, and, accordingly, the intensity in the microchannel is within the range $(3.0-4.5) \times 10^{14}$ W cm^{-2}. It was found that the number of photons per pulse into full solid angle turns out to be $\sim 3 \times 10^5$ photon $\times$ pulses^{-1} sr^{-1}, and the conversion efficiency is $\eta \approx 5 \times 10^{-8}$ (at an incident radiation energy of 800 μJ). We note that the number of photons per pulse is more than an order of magnitude higher than the values recorded at a close intensity value in papers [6, 18].

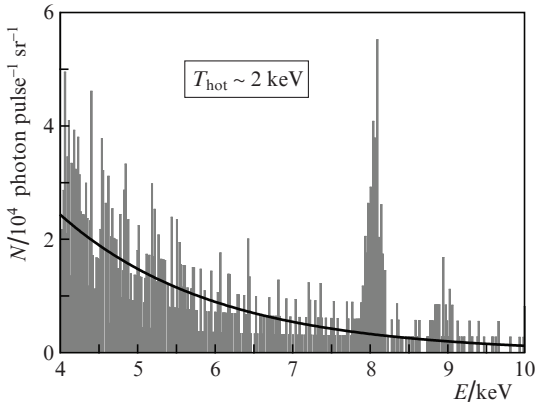

Figure 4. X-ray spectrum of copper in the energy range of 4–10 keV with allowance for the transmittance of air recalculated to the number of photons emitted into a full solid angle at $I \approx (3.2 \pm 0.2) \times 10^{14}$ W cm^{-2}. The full registration time is 15 min.

Based on the measured bremsstrahlung spectrum, we estimated the average energy of hot electrons, which constituted 2 keV. Thus, at moderately low laser intensities, the laser-plasma generation of the bremsstrahlung X-rays and characteristic line of copper occurs due to the hot electronic component. Comparing the known intensity value and energy of hot electrons, we obtain $A = 5.2 \pm 0.3$, which corresponds to the value given in paper [19].

In conclusion, we draw attention to one of the possible practical applications of the results obtained, which is related to the intensity evaluation in a femtosecond filament. It is known that the intensity in a femtosecond filament, which occurs in the air at a laser radiation power exceeding the critical power of self-focusing, can reach 1.4×10^{14} W cm^{-2} [20, 21]. This indicates the possibility of the appearance of X-ray radiation from the laser-induced near-surface plasma initiated by such a filament in the process of ablation of the solid target material. The technique proposed allows evaluation of the filament intensity in measuring the energy of hot electrons from the X-ray bremsstrahlung spectrum. The first results of such measurements will be presented at the conference 'Optics of Lasers 2018'.

4. Conclusions

1. It is found that the threshold radiation intensity of a femtosecond Cr:forsterite laser on the surface of a copper target placed in the air, at which the X-ray generation from the microchannel plasma is recorded, is below the threshold intensity required for X-ray generation from the near-surface plasma and constitutes 0.7×10^{14} W cm^{-2}.

2. Investigated is the dependence of the X-ray yield in the energy range of more than 3 keV from the laser-induced plasma on the laser pulse number with an intensity in the range of $(0.7-4.0)\times10^{14}$ W cm^{-2}, at which there is no nonlinear absorption that significantly affects the delivery of femtosecond laser radiation to the target.

3. The X-ray yield dependence on the laser pulse number is characterised by the presence of an extremum stipulated by reaching a maximum intensity in the conical microchannel. In this case, the X-ray pulse amplitude is approximated by a power-like function, the exponent of which decreases with increasing intensity of the radiation incident on the target.

4. It is established that when femtosecond radiation of a Cr:forsterite laser is softly focused on the surface of a copper target, the laser intensity in the ablated microchannel increases by no more than 2 times compared to the initial value. An increase in the average energy of hot electrons within the framework of refined relation with the intensity of incident radiation does not exceed 1.5 times. In this case, the number of photons per laser pulse into the solid angle constitutes $\sim3\times10^{5}$, and the conversion efficiency is about 5×10^{-8} at a laser pulse energy of 0.8 mJ.

The results obtained can be used to design a simple source of characteristic X-rays of ultrashort duration, to monitor the microchanneling process, and also to derive an estimate of the radiation intensity acting on the target, including the filamentation regime.

Acknowledgements. This work was partially supported by the Russian Science Foundation (Project No. 17-72-20130).

References

1. Ostrikov K.K., Beg F., Ng A. *Rev. Mod. Phys*., **88** (1), 011001 (2016).
2. Sugioka K., Cheng Y. *Light: Sci. Applicat.*, **3** (4), e149 (2014).
3. Labutin T.A., Lednev V.N., Ilyin A.A., Popov A.M. *J. Anal. At. Spectrom*., **31**, 90 (2016).
4. Arora V., Naik P.A., Chakera J.A., Bagchi S., Tayyab M., Gupta P.D. *AIP Advances*, **4**, 047106 (2014).
5. Li C., Cui Y.Q., Zhou M.L., Du F., Li Y., Wang W.M., Chen L.M., Sheng Z.M., Ma J.L., Lu X., Zhang J. *Opt. Express*, **22** (10), 11797 (2014).
6. Hagedorn M., Kkutzner J., Tsilimis G., Zacharias H. *Appl. Phys. B*, **77**, 49 (2003).
7. Gordienko V.M., Makarov I.A., Rakov E.V., Savel'ev A.B. *Quantum Electron*., **35** (6), 487 (2005) [*Kvantovaya Elektron*., **35** (6), 487 (2005)].
8. Gordienko V.M., Zhvania I.A., Makarov I.A. *Laser Phys*., **18** (4), 380 (2008).
9. Pikuz S.A., Chefonov O.V., Gasilov S.V., Komarov P.S., Ovchinnikov A.V., Skobelev I.Y., Ashitkov S.Yu., Agranat M.V., Zigler A., Faenov A.Y. *Las. Part. Beams*, **28** (3), 393 (2010).
10. Zhao X., Shin Y. *Appl. Surf. Sci*., **283**, 94 (2013).
11. Hu W., Shin Y.C., King G. *Appl. Phys. Lett*., **99** (23), 234104 (2011).
12. Hartig K.C., Colgan J., Kilcrease D.P., Barefield J.E., Jovanovic I. *J. Appl. Phys*., **118** (4), 043107 (2015).
13. Zhvaniya I.A., Garmatina A.A., Makarov I.A., Gordienko V.M. *J. Appl. Phys*., **120**, 045901 (2016).
14. Gibbon P., Förster E. *Plasma Phys. Control. Fusion*, **38**, 769 (1996).
15. Klimentov S.M., Garnov S.V., Konov V.I., Kononenko T.V., Pivovarov P.A., Tsar'kova O.G., Brightling D., Dausinger F. *Trudy IOFAN*, **60**, 13 (2004).
16. Gordienko V.M., Khomenko A.S., Makarov I.A., Petukhov V.P. *Laser Phys*., **20** (4), 816 (2010).
17. Gordienko V.M., Lachko I.M., Mikheev P.M., Savel'ev A.B., Uryupina D.S., Volkov R.V. *Plasma Phys. Control. Fusion*, **44** (12), 2555 (2002).
18. Baguckis A., Plukis A., Reklaitis J., Baguckis A., Plukis A., Reklaitis J., Remeikis V., Giniūnas L., Vengris M. *Appl. Phys. B*, **123** (12), 290 (2017).
19. Varanavicius A., Vlasov T.V., Volkov R.V., Gavrilov S.A., Gordienko V.M., Dubetis A., Zeromskis E., Piskarskas A., Savel'ev A.B., Tamosauskas G. *Quantum Electron*., **30** (6), 523 (2000) [*Kvantovaya Elektron*., **30** (6), 523 (2000)].
20. Agranat M.B., Kandidov V.P., Komarov P.S. *Quantum Electron*., **39** (6), 552 (2009) [*Kvantovaya Elektron*., **39** (6), 552 (2009)].
21. Mitryukovskiy S.I., Liu Y., Houard A., Mysyrowicz A. *J. Phys. B: At., Molec. Opt. Phys*., **48** (9), 094003 (2015).